# 2018 SNMMI Highlights Lecture: Cardiovascular Nuclear and Molecular Imaging

*Mehran M. Sadeghi, MD, Yale School of Medicine, New Haven, CT*

*From the Newsline Editor: The Highlights Lecture, presented at the closing session of each SNMMI Annual Meeting, was originated and presented for more than 30 years by Henry N. Wagner, Jr., MD. Beginning in 2010, the duties of summarizing selected significant presentations at the meeting were divided annually among 4 distinguished nuclear and molecular medicine subject matter experts. Each year Newsline publishes these lectures and selected images. The 2018 Highlights Lectures were delivered on June 26 at the SNMMI Annual Meeting in Philadelphia, PA. In this issue we feature the lecture by Mehran M. Sadeghi, MD, a professor in the Department of Internal Medicine (Cardiology) at Yale University School of Medicine (New Haven, CT), who spoke on highlights in cardiovascular nuclear and molecular imaging. Note that in the following presentation summary, numerals in brackets represent abstract numbers as published in* The Journal of Nuclear Medicine *(2018;59[suppl 1]).*

**Mehran M. Sadeghi, MD**

It is a pleasure to be here today to talk about the cardiovascular nuclear and molecular imaging presentations and posters at the 2018 Annual Meeting of the SNMMI. This year's meeting was slightly shorter, but the total number of abstracts in the cardiovascular program remained unchanged from 2017. We had a total of 60 oral presentations and 65 posters. As usual, more than 75% of abstracts were clinical and less than 25% represented the basic sciences. These abstracts came from around the globe, with researchers representing 17 nations. The United States, China, and Japan had the highest numbers of abstracts in the cardiovascular program, comprising almost 75% of presentations.

### State of the Field: What is New This Year?

The breadth and depth of the abstracts in many ways reflect the state of the art in nuclear and molecular imaging and the ways in which this field is influencing the practice of cardiovascular medicine. The general foci of most presentations could be assigned to 1 of 3 categories: (1) those focused on improving the practice of nuclear cardiology through refinement of what we do most, which is myocardial perfusion imaging (MPI); (2) those focused on addressing diagnostic gaps and new applications, such as sarcoidosis, amyloidosis, imaging infection, and imaging vascular inflammation (both in the clinic and as part of preclinical and clinical studies). Applications of nuclear and molecular imaging keep expanding, and new treatments are emerging that may transform patient care and reduce cardiovascular morbidity and mortality. Many of the applications that have emerged in recent years are already incorporated in our daily practice—a testimony to the vitality of the field. This year we had fewer abstracts submitted on infiltrative heart disease, for example, in part because these techniques have matured and transitioned to clinical use. Accordingly, I am sure we will see more clinical trials with these techniques in the near future; and (3) those focused on advancing scientific discovery.

### Cardiovascular Council Young Investigator Award Finalists

The Cardiovascular Council selected a list of outstanding presentations as finalists for this year's Young Investigator Awards. This group of finalists included young investigators who will undoubtedly be future leaders in molecular imaging and nuclear cardiology. Their presentations illustrate the many ways in which the field is advancing. The wide range of both content and countries represented reflect the diversity seen throughout the Annual Meeting. I will discuss the work of a number of these finalists in this lecture but want to congratulate first the 2 Young Investigative Award winners: Anika Hess, from Hannover, Germany, and Takahashi Norikane, from Kagawa, Japan.

Hess and her colleagues from the Medizinische Hochschule Hannover, Scintomics GmbH (Fuerstenfeldbruck), and the Technische Universität München (Garching; all in Germany) studied the kinetics of CXCR4 chemokine receptor expression in a murine model and reported on "CXCR4-targeted imaging of leukocyte mobilization after myocardial infarction (MI)" [37]. This chemokine receptor is expressed on macrophages and other immune cells. We know that MI or ischemia–reperfusion trigger an inflammatory response that mediates wound repair and tissue healing. When it is dysregulated, it leads to abnormal remodeling and even cardiac rupture in extreme cases. These researchers showed that their CXCR4-targeting tracer, $^{68}$Ga-pentixafor,

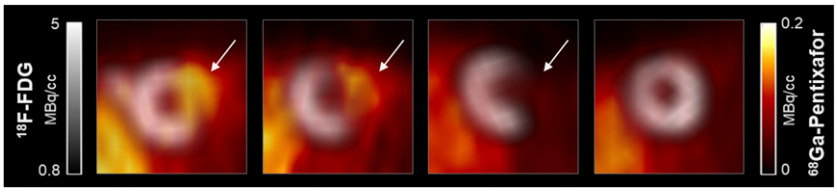


**FIGURE 1.** Early CXCR4 imaging and cardiac outcome. Serial imaging with $^{68}$Ga-pentixafor PET at (left to right, with sham at far right) 1, 3, and 7 days after myocardial infarction (MI) shows CXCR4 upregulation in the infarct territory (arrows; as defined by $^{18}$F-FDG), which is considerably reduced by day 7 post-MI. Mice that died of left ventricular rupture 3–7 days post-MI showed sustained inflammation over the 1–3-day post-MI period compared to survivors. The $^{68}$Ga-pentixafor signal at 1 and 3 days post-MI was inversely correlated to left ventricular ejection fraction at 6 weeks, independent of infarct size.

produced a strong signal at the infarct site at 1 and 3 days postinfarct in mice, with the signal declining by day 7 (Fig. 1). On an interesting note, in animals that died of rupture, this signal remained stable between days 1 and 3, but in animals that survived the signal decreased by day 3. Moreover, they identified an inverse relationship between the pentixafor signal on early post-MI images and left ventricular ejection fraction (LVEF) at a later time point (6 weeks post-MI), independent of infarct size. The researchers then experimented with administration of a CXCR4 antagonist (AMD3100) at 1 hour post-MI. A single dose of this inhibitor reduced LV rupture in these mice and improved late LVEF compared to untreated animals. These studies, which are quite compelling, set the stage for future image-guided therapy of inflammation to improve postinfarct healing.

Takashi Norikane and colleagues from Kagawa University Hospital/Kagawa University (Japan) reported on "Correlation of noninvasive imaging of vulnerable carotid artery plaque using NaF and FDG PET/CT and black-blood MR imaging with cerebral ischemia on brain MR imaging" [40]. In patients with ultrasound-assessed carotid artery stenosis ≥50%, the researchers studied the association between combined carotid artery plaque morphology assessed with MR imaging and plaque biology assessed with $^{18}$F-sodium fluoride ($^{18}$F-NaF) and $^{18}$F-FDG PET/CT imaging (features of vulnerability), and evidence of brain ischemia by MR imaging. In part independent of the degree of stenosis, important structural and biologic features determine the adverse event risk associated with carotid stenosis. These features can be used to define the so-called "vulnerable plaque." The researchers found that the ipsilateral carotid $^{18}$F-NaF signal (reflecting vascular microcalcification)—but not the $^{18}$F-FDG signal (supposedly reflecting inflammation)—was significantly higher in subjects with evidence of more extensive ischemic brain injury. The mean carotid $^{18}$F-NaF $SUV_{max}$ in patients with grade 3 injury (severe brain ischemic change) was significantly higher than that in patients with grade 1 (mild ischemic change) and in patients with grade 2 (moderate ischemic change). No significant association was found between carotid $^{18}$F-FDG $SUV_{max}$, carotid black-blood MR imaging findings, and brain MR imaging ischemic injury grade. Figure 2 is an example from their patient group. The patient has mild ischemic changes on the right side and a more severe lesion on the left. Of note, the right carotid structures visible on carotid black-blood MR imaging were more consistent with the vulnerability, the opposite of what would have been expected. However, the $^{18}$F-NaF signal was markedly stronger on the left side, where there is more brain injury. The mechanistic link here is not clear, but one could assume that this $^{18}$F-NaF signal reflects more embolic events originating from the NaF-positive carotids and therefore identifies plaques that are more prone to thromboembolic events.

### Cardiovascular Council Hermann Blumgart Award

The Cardiovascular Council each year presents the prestigious Hermann Blumgart Award, which recognizes a key contributor to the science of nuclear cardiology who is also an advocate for the field through involvement with the society's research and educational activities. This year's award went to Thomas H. Schindler, MD, an associate professor in the Division of Nuclear Medicine at the Mallinckrodt Institute of Radiology at Washington University in

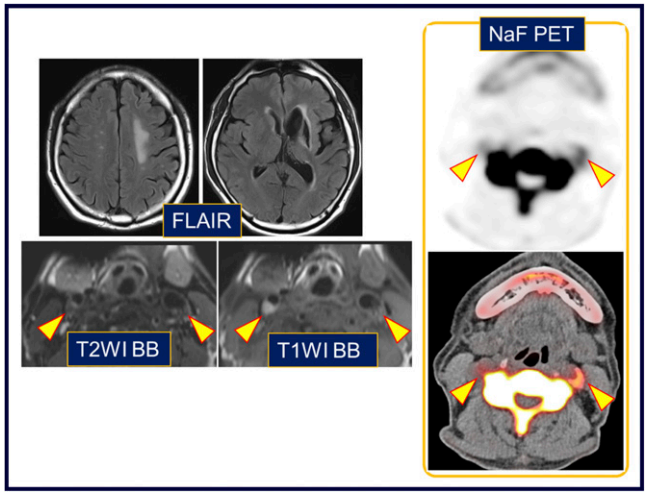


**FIGURE 2.** Correlation of noninvasive imaging of carotid artery plaque using $^{18}$F-NaF and $^{18}$F-FDG PET/CT plus black-blood MR imaging with cerebral ischemia on brain MR imaging. MR images (left) show the presence of mild ischemia on the right side and a more severe lesion on the left. The right carotid plaque shows the features of plaque vulnerability, which is the opposite to what one would expect. On $^{18}$F-NaF PET and PET/CT (right), uptake is markedly higher on the left side, where there is more brain injury. The researchers found that the ipsilateral carotid $^{18}$F-NaF signal (reflecting vascular microcalcification) but not the $^{18}$F-FDG signal (supposedly reflecting inflammation) was significantly higher in subjects with evidence of more extensive ischemic brain injury.

St. Louis, MO. At the award ceremony, he presented a lecture on the role of cardiac PET in in vivo assessment of cardiovascular disease and the importance of this role in contemporary and future cardiovascular medicine.

### Technologic and Methodologic Advances in MPI

A number of important abstracts at the Annual Meeting focused on what I would call refining the "bread and butter" of nuclear cardiology—MPI. MPI is the workhorse of what we do in our labs, and this is likely to remain true for some time into the future. Some of these refinements are technologic and methodologic advances, such as those in image analysis (including improving myocardial blood flow [MBF] and coronary flow reserve [CFR] measurements), as well as motion correction techniques. Although the meeting featured many outstanding presentations, time constraints allow me to review only a few representative examples. My apologies go to the authors of the many cardiovascular-related presentations not included here.

One example of work being done in this area is that of Katoh et al. from Hokkaido University/Hokkaido University School of Medicine (Sapporo, Japan), who looked at the role of cardiac gating in image analysis of $^{15}O$-$H_2O$ PET/CT. They reported on a "Strategy to improve the detectability of CFR in the ischemic myocardial lesion with ECG-gated dynamic myocardial PET with $^{15}O$-$H_2O$: Comparison with conventional nongated PET" [435]. Gating led to a reduction in stress MBF and CFR in ischemic segments but had no effect on segments with normal perfusion, potentially improving the detectability of ischemic changes. They concluded that gating can improve the accuracy of MBF measurements in the presence of ischemia.

Today MBF measurements are incorporated in our daily practice. Although this improves the accuracy of perfusion imaging, the process of deriving and using these metrics remains challenging, with many potential pitfalls and error-prone steps. Under Dr. deKemp's direction, a Canadian group developed a simplified method to estimate myocardial flow reserve (MFR) from late static flow rest and stress images. Wu et al. from the Centre Hospitalier de l'Universite de Montreal, Queen's University School of Medicine (Kingston), and the University of Ottawa Heart Institute (all in Canada) reported on "Simplified estimation of MFR using stress/rest activity ratios with $^{13}N$-ammonia and $^{82}Rb$ PET" [433]. They defined a myocardial activity ratio (obtained from late static images) and showed good correlation between MFR from dynamic images and the myocardial activity ratio. In fact, this ratio was able to accurately distinguish patients with abnormal flow reserve. Another advantage to this approach is that these static images might be used for exercise PET studies, which cannot currently be used for MFR assessment. The authors concluded that their simplified approach has the potential to remove the need for dynamic imaging and tracer kinetic modeling in this setting.

Another area of technologic and methodologic advances in our field is in automation and artificial intelligence. At this meeting we saw some very nice presentations on automated analysis of MPI and on machine learning to improve MPI analysis. Otaki et al. from Cedars–Sinai Medical Center (Los Angeles, CA), Assuta Medical Centers (Tel Aviv, Israel), Brigham and Women's Hospital (Boston, MA), Sacred Heart Medical Center (Springfield, OR), and the University of Ottawa Heart Institute (Canada), under Dr. Slomka, reported on the "Prognostic value of quantitative high-speed MPI in a multi-center study" [505]. This group of researchers assembled a registry database of more than 150,000 MPI studies performed on cadmium-zinc-telluride SPECT cameras, incorporating clinical data and, in some cases, coronary angiography results. The database is called REFINE (REgistry of Fast Myocardial Perfusion Imaging with NExt generation SPECT). Participants had undergone either exercise or pharmacologic stress $^{99m}Tc$-sestamibi high-speed MPI and were followed for 3.2 ± 1.6 years for adverse major cardiac events. As one of many studies underway, the researchers looked at a fully automated analysis of stress-only images and compared these data with visual reads of rest and stress images with regard to major adverse cardiac events. They found that these events increased progressively with increasing perfusion abnormality among patients undergoing stress, and that several differences characterized groups of men and women with the same quantitative MPI results. A fully automated quantitative analysis of stress-only images provided additional information to the conventional reads of stress and rest images and could identify some patients with higher propensity for major cardiac events. Quantitative analysis allowed precise granular risk stratification in comparison to visual reading, even for cases with normal clinical readings. These results also suggest that visual reads of stress/rest studies and automated quantitative analysis of stress-only scans may have complementary roles, highlighting subtle defects.

The same collaborative research group used images and data to develop and test a deep learning algorithm. Betancur et al. from Cedars–Sinai Medical Center (Los Angeles, CA), Assuta Medical Centers (Tel Aviv, Israel), Brigham and Women's Hospital (Boston, MA), Cardiovascular Imaging Technologies LLC (Kansas City, MO), Columbia University Medical Center (New York, NY), Sacred Heart Medical Center (Springfield, OR), University Hospital Zurich (Switzerland), University of Ottawa Heart Institute (Canada), and Yale University/Yale University School of Medicine (New Haven, CT) reported on "Automatic deep learning analysis of upright-supine high-speed SPECT MPI for prediction of obstructive coronary artery disease (CAD): A multicenter study" [507]. The researchers studied a subset of 1,159 CAD patients from 4 different centers, who underwent stress $^{99m}Tc$-sestamibi MPI with new-generation solid-state SPECT scanners. All patients underwent invasive coronary angiography for correlation within 6 months of MPI. Deep learning based on acquired data was used to score the probability of obstructive CAD. Per-patient disease probability was calculated. Data from 3 of the centers was

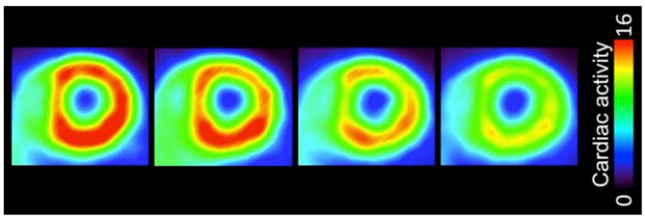


**FIGURE 3.** $^{11}$C-HED PET uptake in the rat heart. Representative dynamic axial $^{11}$C-HED PET images with different tracer-specific activities (left to right: 0.2, 1, 10, and 34 μg/kg) acquired 25–30 minutes after injection showed rapid blood clearance and clear delineation of the myocardium in all animals, with a dose-dependent reduction in tracer uptake.

used for training, and the remaining center was used for evaluation. Predictions for each center were integrated to yield an overall estimation of the multicenter performance. They showed that this deep learning system algorithm performed slightly better for detection of obstructive CAD than traditional reading by experts.

### Accelerating Scientific Discovery

Many of the abstracts that were presented this year focused on addressing important aspects of cardiovascular pathophysiology, and together they highlight the critical role of nuclear and molecular imaging in advancing scientific discovery. One example came from Werner et al. from the Johns Hopkins University School of Medicine (Baltimore, MD), the National Cardiovascular and Cerebral Research Center (Osaka, Japan), and the University of Würzburg (Germany), who reported on "The impact of aging on [$^{11}$C]meta-hydroxyephedrine ($^{11}$C-HED) uptake in the rat heart" [100]. In a carefully designed rat study, Dr. Werner and colleagues evaluated how the timing of $^{11}$C-HED utilization after tracer production affects the myocardial signal and image quality. $^{11}$C-HED is often used to assess sympathetic innervation in the myocardium, and these authors worked to identify some of the confounding factors in the signal generated by the tracer. This is quite important, because such techniques, with this or other tracers, will one day be routinely available in the clinic to help us identify patients with heart failure who are at risk for sudden death. The researchers injected the tracer with increasing amounts of cold mass in rats (Fig. 3) and observed dose-dependent reduction in retention index (a marker of norepinephrine reuptake function) and, thus, specific uptake of $^{11}$C-HED in the heart. In the second part of this study, the authors addressed a physiologic question: does aging have an impact on myocardial $^{11}$C-HED uptake? Animals were imaged serially from 2 to 15 months, over which time period a gradual decrease in $^{11}$C-HED signal was noted in the normal myocardium (Fig. 4). The $^{18}$F-FDG signal, however, was not affected by aging. The biologic basis and implications of this interesting observation remain to be determined, but if this same phenomenon can be observed in humans, this could be a very important confounding factor for future consideration.

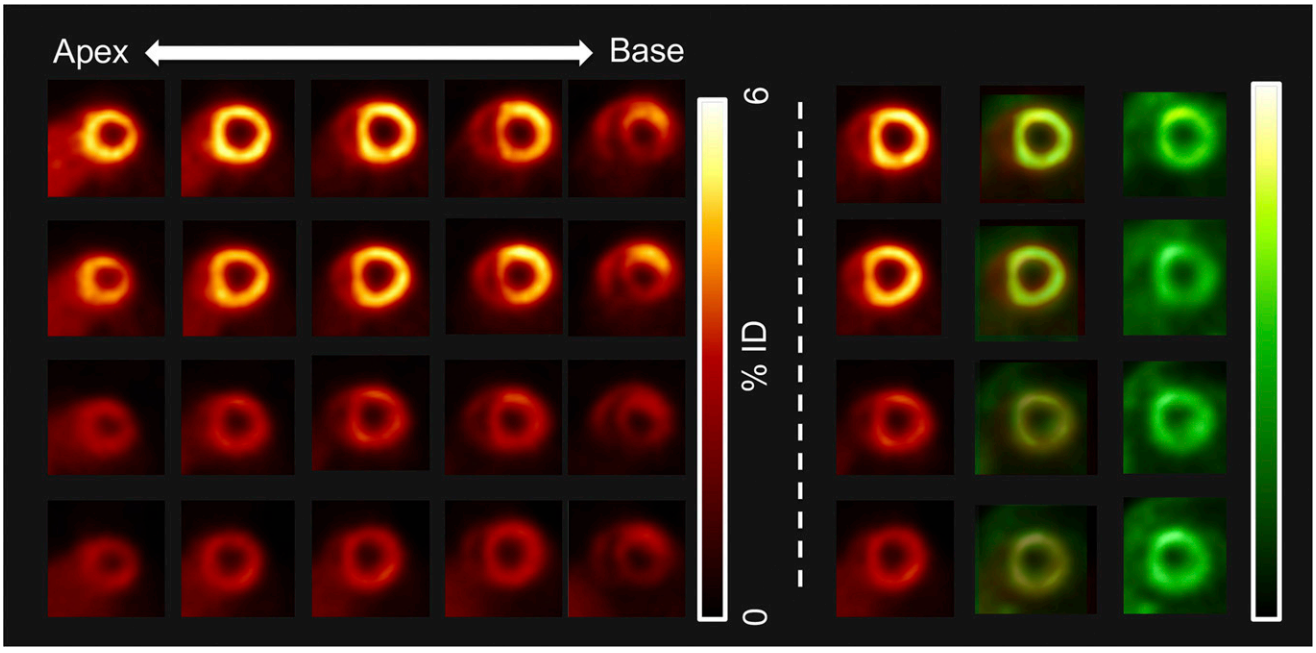


**FIGURE 4.** Impact of aging on myocardial $^{11}$C-HED uptake. In a longitudinal setting, serial $^{11}$C-HED imaging was conducted at different ages in Wistar rats. $^{11}$C-HED PET images (left block) at (top to bottom) 2, 5, 11, and 15 months show clear visualization of the left ventricular wall, indicating high and homogeneous tracer activity throughout the left ventricular myocardium for all animals at month 2. However, the homogeneous cardiac uptake pattern reduced subsequently from months 5 to 11, and further decline could be detected at month 15. Right block, left to right: $^{11}$C-HED, fused images, and $^{18}$F-FDG images at the same timepoints. $^{18}$F-FDG uptake remained stable throughout the ventricle at different ages, indicating preserved myocardial viability.

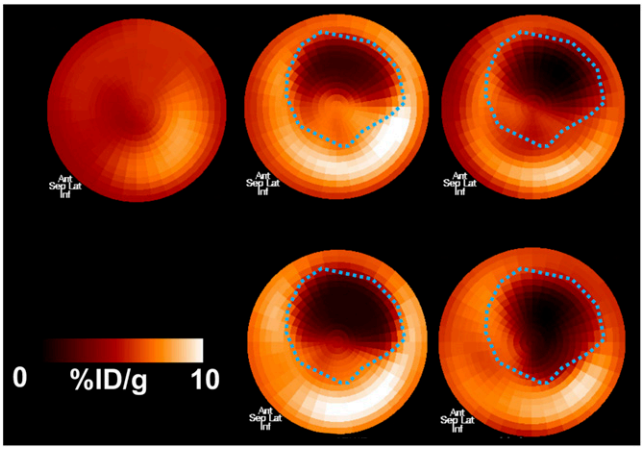


**FIGURE 5.** Cardiac translocator protein (TSPO) signal modulated by enalapril therapy after myocardial infarction (MI). Top row, left to right, at 1 week after MI: sham imaging, $^{18}$F-GE180 uptake without enalapril administration, and $^{18}$F-GE180 uptake on enalapril therapy. Bottom row, at 8 weeks after MI: $^{18}$F-GE180 uptake without enalapril administration and $^{18}$F-GE180 uptake on enalapril therapy.

MI is associated with systemic inflammation. Several recent studies have shown evidence of neuroinflammation in the post-MI period. Borchert et al. from the Medizinische Hochschule Hannover (Germany) reported on "Dissecting the heart/brain interaction in postinfarct myocardial inflammation by whole-body translocator protein (TSPO) imaging" [102]. Using the tracer $^{18}$F-GE180 to detect the extent of inflammation in the postinfarct period in a murine model, they showed that the cardiac TSPO signal from this tracer increased at 1 and at 8 weeks post-MI. They also demonstrated that this signal may be reduced by administration (beginning 3 days before coronary artery occlusion until 7 days post-MI) of the angiotensin-converting enzyme (ACE) inhibitor enalapril (Fig. 5). The ACE inhibitor lowered global cardiac TSPO signal at day 7, possibly by preventing splenic mobilization of leukocytes. Measuring cardiac function by electrocardiograph-gated $^{99m}$Tc-sestamibi perfusion SPECT showed that the ACE inhibitor treatment led to better LVEF at 8 weeks after MI. Increased $^{18}$F-GE180 uptake was observed in the brain at 1 and 8 weeks after MI, with good correlation between tracer uptake in the heart and the brain, suggesting an association between heart and brain inflammation (Fig. 6). The enalapril effect on brain signal, however, was observed at 1 week but not at 8 weeks post-MI. The clinical significance of neuroinflammation after MI, as well as the chronic effect of enalapril on neuroinflammation and associated implications for development of cognitive impairment remain to be determined.

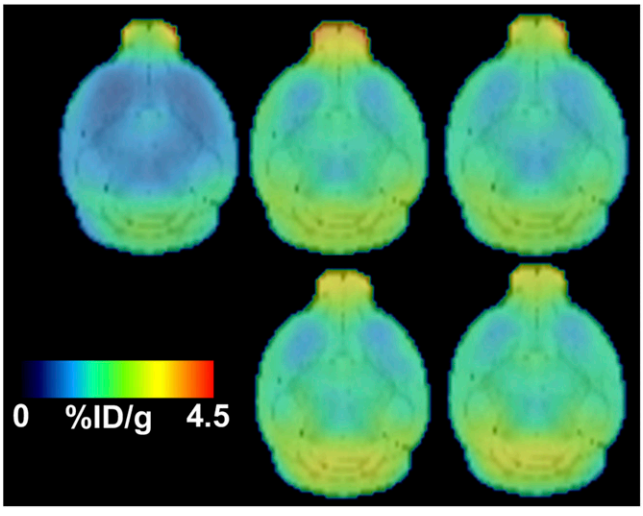


**FIGURE 6.** Brain translocator protein (TSPO) signal modulated by enalapril therapy after myocardial infarction (MI). Serial imaging with $^{18}$F-GE180 targeting TSPO showed that preventative enalapril treatment lowered global brain TSPO signal at day 7 post-MI (top row, left to right: in sham, untreated, and enalapril-treated mice). At 8 weeks post-MI (bottom row, untreated and enalapril-treated mice) uptake differences were not apparent.

Continuing on the theme of brain interaction with the cardiovascular system, our group has been interested in posttraumatic stress disorder (PTSD), which is associated with increased cardiovascular morbidity and mortality. Toczek et al. from the Veterans Affairs Connecticut Healthcare System (West Haven) and the Yale University School of Medicine (New Haven, CT) reported on "FDG PET imaging of vascular and systemic inflammation in patients with PTSD" [302]. We looked at the $^{18}$F-FDG signal in patients with PTSD (Fig. 7) and in control patients who were imaged over a 2-hour period. Tracer signal in the ascending aorta was quantified on images in the last 30 minutes and was expressed as target-to-background ratio by normalizing the average $SUV_{max}$ measured on consecutive slices with blood pool activity ($SUV_{mean}$) measured in the superior vena cava. No measurements of vascular or systemic inflammation differentiated PTSD and control subjects, as assessed by FDG PET imaging. Although we did not detect a correlation between vascular and brain

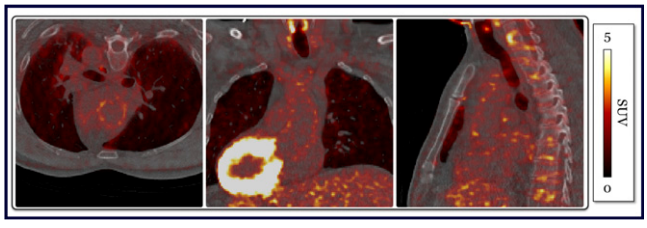


**FIGURE 7.** $^{18}$F-FDG PET imaging of vascular and systemic inflammation in patients with posttraumatic stress disorder (PTSD). $^{18}$F-FDG signal in the ascending aorta was quantified on images acquired at 90 minutes and was expressed as target-to-background ratio by normalizing average maximal standardized uptake values measured on consecutive slices, with blood pool activity ($SUV_{mean}$) measured in the superior vena cava. On the same late images, $^{18}$F-FDG uptake was quantified in the spleen, bone marrow and brain region of amygdala and expressed as $SUV_{mean}$. No measurements of vascular or systemic inflammation differentiated PTSD and control subjects, as assessed by $^{18}$F-FDG PET imaging.

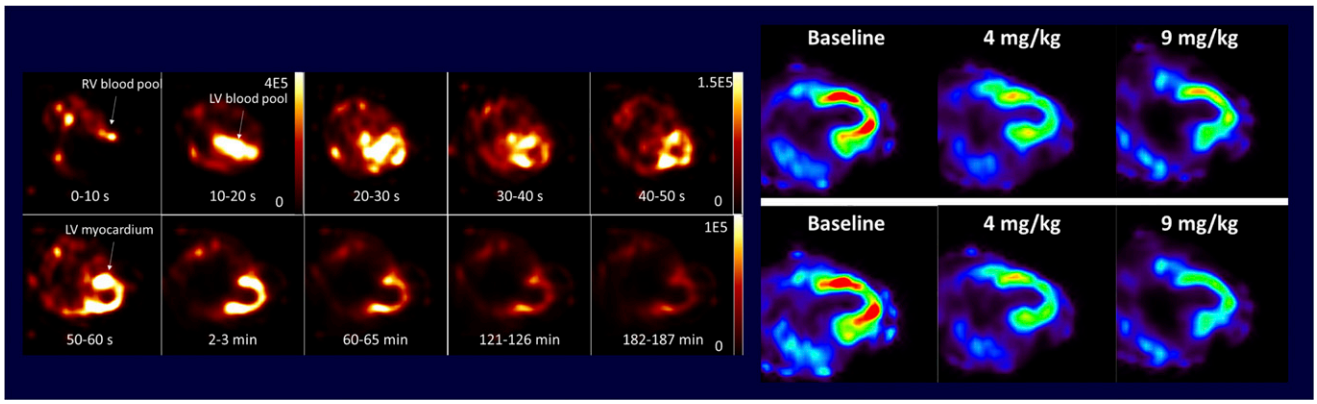


**FIGURE 8.** Dynamic $^{123}$I-MIBG SPECT for early detection of doxorubicin-induced cardiotoxicity in dogs. Left block: Dynamic $^{123}$I-MIBG SPECT images at 8 mg/kg doxorubicin at (top, left to right) 0.20, 10–20, 20–30, 30–40, and 40–50 seconds and (bottom, left to right) 50–60 seconds and 2–3, 60–65, 121–126, and 182–187 minutes. Right block: Static (top row) and $V_T$ (bottom row) myocardial uptake of $^{123}$I-MIBG at (left to right) baseline, 4 mg/kg, and 9 mg/kg doxorubicin.

$^{18}$F-FDG signal, a significant correlation was found between tracer signal in the spleen and bone marrow, and uptake in both tissues correlated with uptake in the amygdala. This suggests interaction between systemic and central nervous system inflammation. The study was initially conducted in a small number of patients and needs to be extended.

Dr. Dorbala's group from Boston looked at myocardial energetics in cardiac amyloidosis, which is associated with heart failure and potential changes in myocardial metabolism. In this study, El-Sady et al. from the Brigham and Women's Hospital (Boston, MA) reported on "Myocardial energetics in AL (light chain) and ATTR (transthyretin-related) cardiac amyloidosis: An $^{11}$C-acetate PET/CT study" [228]. The study included 20 patients with AL cardiomyopathy and 3 with ATTR cardiomyopathy, who underwent $^{11}$C-acetate PET/CT and echocardiography. Their results showed that $k_{mono}$, a measure of myocardial metabolism, is lower in ATTR amyloidosis than in AL. However, after correcting for myocardial work, myocardial energy efficiency is better in ATTR. This raises some potential for novel therapeutics to manipulate substrate utilization in AL cardiomyopathy.

### Expanding the Horizon

Investigators continue to expand the diagnostic and therapeutic horizons of our field by introducing new applications, tracers, and methodologies for nuclear cardiology. New applications were reported at this meeting in cardiotoxicity, erectile dysfunction, carotid stenosis, and in Anderson–Fabry disease, among others. New tracers include $^{18}$F-HX-01 for flow, 6″-$^{18}$F-fluoromaltotriose for endocarditis, $^{18}$F-florbetapir for cardiac amyloidosis, and $^{99m}$Tc-rhAnnexin V-128 for apoptosis in atherosclerosis. Among the new methodologies are innovations in coronary $^{18}$F-NaF uptake quantification.

As an example of a new application, Wu et al. from Yale University (New Haven, CT) and Weill Cornell Medical

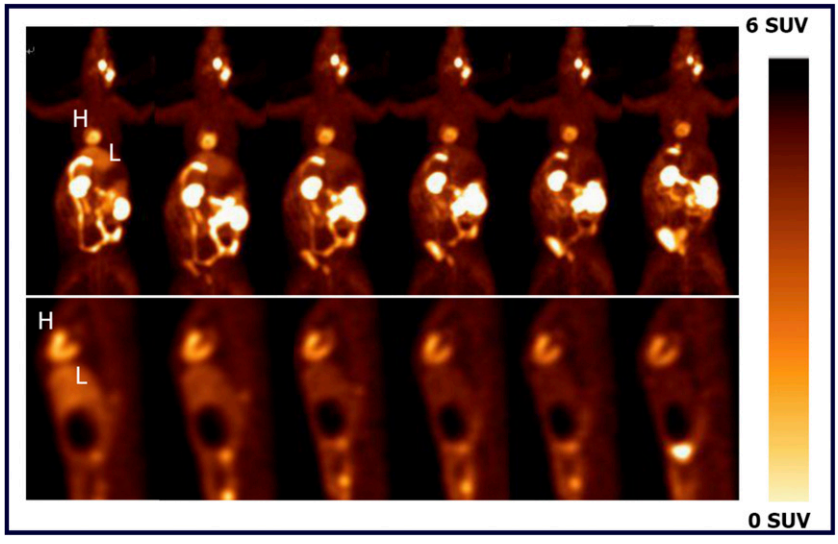


**FIGURE 9.** Radiosynthesis and biologic evaluation of $^{18}$F-HX-01 for cardiac PET. Frontal multiple-intensity projection (top) and sagittal (bottom) PET/CT images of $^{18}$F-HX-01 in a healthy New Zealand white rabbit acquired at (left to right) 10, 30, 45, 60, 75, and 120 minutes after injection.

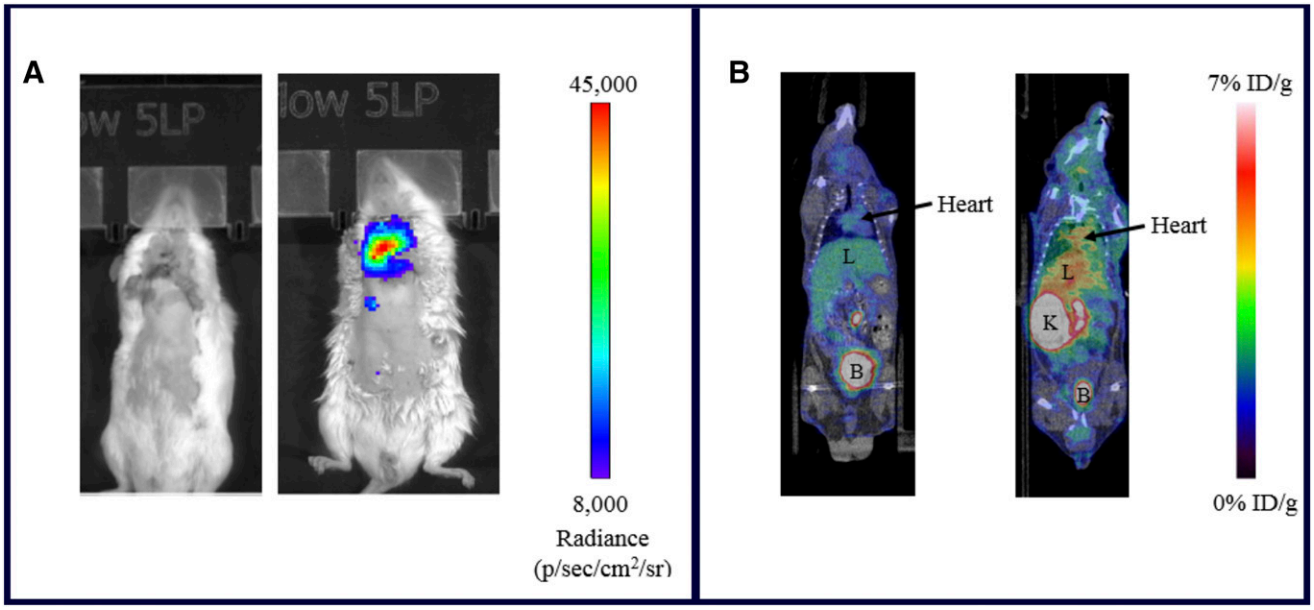


**FIGURE 10.** Molecular imaging of cardiovascular infections with 6"-$^{18}$F-fluoromaltotriose PET/CT. Bioluminescence imaging (BLI, left) and PET/CT imaging (right) in controls (left in each image) and mice with *staphylococcus aureus* endocarditis (right in each image). The tracer is taken up by gram-positive and -negative bacteria but not by mammalian cells. Both BLI and PET signals in the heart region of the infected mouse are high. The researchers observed ~2.5-fold higher mean tracer uptake in infected mice hearts when compared to control mice. Arrows, heart; L = liver; K = kidneys; B = bladder.

College (New York, NY) reported on "Dynamic SPECT imaging of $^{123}$I-MIBG for early detection of doxorubicin-induced cardiotoxicity in dogs" [101]. With no reliable technique for early detection, accurate identification of cardiotoxicity remains an important diagnostic gap in cardiology. The technique used by this group calculated voxel-by-voxel volume of distribution ($V_T$), which is defined as the ratio of tracer activity concentration in the myocardium to that in the plasma at equilibrium. Seven dogs received weekly doxorubicin (1 mg/kg/week) to achieve 15 mg/kg cumulative dose or until LVEF was <45%. Results showed that myocardial uptake of $^{123}$I-MIBG decreased with cumulative doxorubicin dose in both static and $V_T$ images (Fig. 8). Of note, the changes in $V_T$ preceded changes in ejection fraction in these dogs, suggesting that dynamic SPECT imaging of $^{123}$I-MIBG may be used as an effective tool in the early detection of doxorubicin-induced cardiotoxicity.

One of the new tracers presented in the meeting was an $^{18}$F-based mitochondrion-targeting agent for flow imaging. Wang et al. from the West China Hospital of Sichuan University (Chengdu) reported on "Radiosynthesis and biological evaluation of a novel berberine derivative for cardiac PET imaging" [35]. In a rabbit model, they demonstrated good cardiac uptake, early clearance, and good contrast between the heart and the liver. Dynamic PET/CT images of $^{18}$F-HX-01 in healthy rabbits (Fig. 9) showed good visualization of the heart at 10 minutes postinjection, and the radioactivity was retained in the heart at a high level up to 120 minutes. Higher myocardium-to-liver and myocardium-to-lung activity ratios were obtained at 30 minutes postinjection, making it possible to acquire PET data earlier after injection and indicating that $^{18}$F-HX-01 could be a promising cardiac imaging agent. These kinds of tracers may facilitate exercise PET MPI, which is not currently feasible with $^{82}$Rb.

Wardak et al. from Stanford University School of Medicine (CA) reported on "Molecular imaging of cardiovascular infections with 6″-[$^{18}$F]-fluoromaltotriose PET/CT" [36], a new technique for identifying endocarditis. This novel PET tracer is transported via a system that is exclusive to bacteria and not present on mammalian cells. Their study showed that this tracer is taken up by gram-positive and -negative bacteria but not by mammalian cells. Using a murine model of *staphylococcus aureus* endocarditis, they showed a 2.5-fold increase in tracer uptake in endocarditis over uptake in control animals. The 6″-$^{18}$F-fluoromaltotriose agent was able to image valvular infection with high sensitivity and specificity (Fig. 10), with the potential to change the clinical management of patients suffering from infectious diseases of bacterial origin. The researchers are planning to translate this tracer into the clinic, addressing an important diagnostic gap in cardiovascular medicine.

## Conclusion

Our field is thriving with many refinements to perfusion imaging, new applications, and new tracers. Some of the new applications introduced in previous years are now fully integrated into clinical practice. Several innovations in the pipeline are expected to expand the utilization and value of nuclear and molecular imaging in cardiology.